

Document downloaded from:

<http://hdl.handle.net/10251/140414>

This paper must be cited as:

Orts, F.; Bonastre, J.; Fernández, J.; Cases, F. (20-1). Effect of chloride on the one step electrochemical treatment of an industrial textile wastewater with tin dioxide anodes. The case of trichromy Procion HEXL. *Chemosphere*. 245:1-7.
<https://doi.org/10.1016/j.chemosphere.2019.125396>



The final publication is available at

<https://doi.org/10.1016/j.chemosphere.2019.125396>

Copyright Elsevier

Additional Information

1 **Effect of chloride on the one step electrochemical treatment of an industrial textile**
2 **wastewater with tin dioxide anodes. The case of trichromy Procion HEXL**

3

4 F. Orts, J. Bonastre, J. Fernández and F. Cases*

5 Departamento de Ingeniería Textil y Papelera, Escuela Politécnica Superior de Alcoy,
6 Universitat Politècnica de València. Plaza Ferrándiz y Carbonell, s/n, 03801, Alcoy, Spain.

7

8

9 **ABSTRACT**

10

11 The resulting solutions from the cotton fabrics dyeing using the trichromy Procion
12 HEXL, with NaCl as electrolyte, were electrochemically treated. These dyes have two
13 azo groups as chromophores and two monochlorotriazinic groups as reactive groups in
14 their structure. The combined oxidation/reduction at 125 mA cm^{-2} in a filter-press cell
15 without compartment separation was carried out using an anode of Ti/SnO₂-Sb-Pt and a
16 cathode of stainless steel. This procedure has been effective in previous experiments
17 using sulphate as electrolyte. A significant decrease in total organic carbon (TOC),
18 chemical oxygen demand (COD), and total nitrogen (TN) was obtained. Moreover, the
19 process took place efficiently. The average oxidation state (AOS) and the carbon
20 oxidation state (COS) data confirmed the presence of stable oxidized intermediates in
21 the electrolysed solution. The chromatography and the UV-Visible spectrophotometry
22 assays indicated that full decolourisation is obtained at a loaded charge of around 0.81
23 Ah L⁻¹ which is associated with an electrical energy per order (EEO) of 1.20 kWh m^{-3} .

24

25

26

27

28

29

30

1 **Keywords:** Tin dioxide anodes, electrochemical treatment, dyestuff wastewater,
2 trichromy, chloride.

3
4 * *To whom correspondence should be addressed.*

5 *Telephone: +34.96.652.84.12*

6 *Fax: +34.96.652.84.38*

7 *e-mail: fjcases@txp.upv.es (F. Cases)*

8
9

10 **1. Introduction**

11

12 In environmental terms, the textile industry generates a great deal of solid, gaseous
13 and contaminated wastewater (Drumond Chequer et al., 2013; Lacasse, 2004). But, it is
14 in wastewater pollution that the textile sector has the greatest environmental impact
15 (Ghaly, 2014; Shukla, 2007). Research into treatments to bleach and degrade colouring
16 agents in textile wastewater is currently an important topic of study in the textile
17 industry.

18

19 Generally, wastewater discharged from dyestuff is characterized by colour, BOD,
20 COD, pH, and salinity (Blanco et al., 2014; De Jager et al., 2014). Pollution by
21 discharges of dyes occurs because part of the dye present in dyestuff baths is not fixed
22 to the textile fibre and then, passes to effluents. The ability to fix the dye to the fibre
23 varies depending on the nature of the dye and the type of dye process. Reactive dyes
24 have a particularly low percentage of fixation (European Commission, 2005). These dyes
25 are mainly used in cotton dyestuff and the consumption of these represents
26 approximately 20-30% of the total consumption of dyes (Carneiro et al., 2005). The

1 reaction between the fibre and dye takes place at an alkaline pH. Under these
2 conditions, the dye also reacts with the water giving rise to a competitive reaction of
3 hydrolysis. In this process, part of the dye is not fixed to the fibre, so that, once the
4 dyestuff is finished, the resulting bath contains dye in its hydrolyzed form that can no
5 longer be fixed to the fibre.

6

7 To improve the performance of these dyestuffs, bifunctional reactive dyes have been
8 developed. This type of dyes presents two reactive groups in their structure with which
9 the percentage of dye that reacts with the fibre is significantly increased. The percentage
10 of fixation of a monofunctional reactive dye is around 60%, and in the case of a
11 bifunctional reactive dye, it increases to values of around 80% (Allen, 1971). Therefore,
12 the use of bifunctional reactive dyes leads to a reduction in the amount of dye
13 discharged with the effluent. Nevertheless, this poor performance means that much of
14 the dye used is discharged in its hydrolyzed form (Guaratini et al., 2001a, 2001b).

15

16 The presence of dyes in natural water resources strongly colours the water since
17 small concentrations of dyes (of the order of mg L^{-1}) can produce a significant
18 colouring. This produces not only an unpleasant visual effect but also prevents that light
19 reach to the beds of natural waters, with consequent damage to flora and fauna. In
20 addition, colouring of these wastewaters prevents direct reuse.

21

22 In recent years, increasingly effective methods of removing contaminants from
23 textile wastewater have been developed. The main objective of these methods is to
24 achieve the highest possible mineralization or, at least, to produce less aggressive
25 intermediates for the environment. Therefore, the ideal treatment is one that does not

1 generate any additional polluting waste that persists in the environment and,
2 furthermore, that is as economical as possible (Brillas and Martínez-Huitle, 2009;
3 Miklos et al., 2018)

4

5 The use of electrochemical treatments (Brillas and Martínez-Huitle, 2015; García
6 Segura et al., 2018; Ling et al., 2016; Moreira et al., 2017; Sala and Gutiérrez Bouzán,
7 2014) achieved complete decolourisation. It is reported in the bibliography that these
8 objectives are strongly conditioned by the presence and concentration of chloride in the
9 treated effluent (Chatzisymeon et al., 2006; Malpass et al., 2007). It is reported that in
10 some cases the addition of sodium chloride in concentrations of up to 0.1 M allows total
11 decolourisation and an important increase of COD abatement (Malpass et al., 2007;
12 García Segura et al., 2018). Moreover, the effluent conductivity, the applied current
13 density, and the anode material influence the power consumption. In general, it is
14 reported that anodes such as boron doped diamond (BDD) reduce COD and TOC in a
15 shorter operation time and energy consumption ranged between 16 and 100 kWh m⁻³
16 (Ling et al., 2016; Martínez-Huitle et al., 2012).

17

18 In previous works (Orts et al., 2018, 2019), the electrochemical treatment of a real
19 dyestuff wastewater using Na₂SO₄ as electrolyte was carried out. Ti/SnO₂-Sb-Pt non-
20 active anodes were used. Under these conditions, the ·OH radicals are the main
21 electroactive species physisorbed on the anode surface. A complete decolourisation was
22 obtained in the successive reuses of treated wastewater. Moreover, a significant
23 incineration of organic molecules into CO₂ was obtained. It was concluded that the
24 electrochemical treatments saved consumption of water and electrolyte (up to 70%)
25 since the reuse of wastewaters (from the dyeing baths) prevents the discharge into the

1 environment of this effluents charged with a high content of salts. Nevertheless, energy
2 consumption, current efficiency, and electrochemical mineralization must be improved.
3 For these purposes, the use of chloride as electrolyte is examined in the present work. In
4 addition, it should be noted that sodium chloride is the preferred electrolyte in the textile
5 industry for cotton dyeing processes with reactive dyes. The main hypothesis of the
6 present work is that the electrogeneration of active chlorine species for the indirect
7 electrooxidation of real dyestuff wastewater would resolve the weaknesses of previous
8 electrochemical treatments.

9

10 **2. Experimental**

11 *2.1 Reagents, materials and dye procedure*

12 Solutions obtained from the dyestuff baths of cotton fibres with bifunctional reactive
13 dyes belonging to the trichomy Procion HEXL were used for the study. The molecular
14 structures of the dyes of the trichomy Procion HEXL (Yellow, Crimson and Navy) are
15 shown in Fig. 5. Their C.I. name or CAS number of the European Chemicals Agency
16 are: Reactive Yellow 138:1, Reactive Red 231, and 190914-23-9 (C.I. name non-
17 registered), respectively. The dyes were supplied by Dystar Company (Singapore).

18 The initial concentration of each dye was 0.50 g L^{-1} . As electrolyte, NaCl or Na_2SO_4
19 (Fluka quality of analysis) was used in a concentration of 32.0 g L^{-1} or 45.0 g L^{-1} ,
20 respectively, with a specific conductivity of around 42 mS cm^{-1} . The initial pH of the
21 solution was 7. This pH has to be raised during the dyestuff (in the dye fixation process)
22 to an interval between 10.8 and 11.0 by the addition of NaOH.

23

1 For the dyeing procedure, seven stainless steel test tubes (40 mm diameter and 160
2 mm height) containing 125 mL of a 0.5 g L⁻¹ solution of each dye, 10 g of semi-milled
3 cotton fabric 100% (the cotton fabric is previously washed with a solution of H₂O₂ and
4 NaOH) are prepared. The liquor ratio is 1:12.5 (g fabric mL dye⁻¹) and a percentage of
5 dye in relation to the fabric of 1.87 (g dye g fabric⁻¹). These test tubes are placed in a
6 RED-TEST equipment (UNGOLINI RT-P). For the dyestuff procedure, the initial
7 temperature of 15 °C was increased, following a 1.5 °C min⁻¹ gradient, up to 80 °C.
8 About 60 min later, a pH=10.8 was adjusted with a NaOH solution. The dyeing process
9 continued for about 120 min.

10 NaOH, H₂O₂ and HCl (quality of analysis) were supplied by the company Fluka.
11 Distilled water (5.3 μS cm⁻¹) was used for the preparation of the solutions.

12

13 *2.2 Electrolysis*

14 The bath solutions obtained after dyeing process were electrochemically treated in
15 galvanostatic conditions applying a current density of 125 mA cm⁻² in a filter press cell
16 without compartment separation. The choice of this electrochemical conditions was
17 based on previous researches carried out with various reactive dyes (del Río et al.,
18 2009a, 2009b, 2012).

19 The volume of the treated solution and the flow rate were 0.45 L and 5.60 L min⁻¹,
20 respectively. The temperature during the electrolysis was 40°C. The pH of the treated
21 solutions started with values close to 11.0 and decreased until values close to 7.0 at the
22 end of the electrolysis. During the course of electrolysis, samples were extracted to
23 evaluate the decolourisation and the degradation of the remaining hydrolyzed dyes in
24 the dyestuff baths. The anode used was an electrode type DSA of Ti/SnO₂ doped with
25 Sb and with small amount of Pt obtained by pyrolysis of the salts of Sn, Sb and Pt on a

1 substrate of titanium as described in (Orts et al., 2018). The results obtained by our
2 research group during the development of previous projects, have demonstrated the
3 efficiency of the use of these anodes in the decolourisation/degradation of reactive dye
4 solutions (Sala et al., 2012). The incorporation of platinum provides high stability to the
5 anode thus extending its useful life (del Río et al., 2010). The cathode is made of 11.0
6 cm x 9.5 cm stainless steel (Cr 18-19% and Ni 8.5-9%) which was pretreated and
7 cleaned. These pretreatments consist of mechanical polishing and degreasing in an
8 acetone bath subjected to the action of ultrasound in order to eliminate surface fats and
9 oxides. A Grelco GVD310 0-30Vcc/0-10 UNA power supply was used for the control
10 and measurement of the applied current under galvanostatic conditions.

11 *2.3 Analysis and instruments*

12 The degree of degradation of the dyes was evaluated by measurements of total
13 organic carbon (TOC), chemical oxygen demand (COD), and total nitrogen (TN). The
14 average oxidation state (AOS) was obtained from the equation (1) (Bilińska et al., 2016;
15 Clesceri L. S., Eaton, A. D., 1995; Stumm and Morgan, 2013),

16

$$17 \quad \text{AOS} = 4 \cdot (\text{TOC}_t - \text{COD}_t) / \text{TOC}_t \quad (1)$$

18

19 The carbon oxidation state (COS) (Comninellis and Pulgarin, 1991) and the average
20 current efficiency (ACE) (Akrouf and Bousselmi, 2012; Fóti and Comninellis, 2010;
21 Jarrah and Mu'azu, 2016; Xu et al., 2016; Li et al., 2017) were calculated by means of
22 the equations (2) and (3).

23

$$24 \quad \text{COS} = 4 \cdot (\text{TOC}_0 - \text{COD}_t) / \text{TOC}_0 \quad (2)$$

$$ACE=100 \cdot F \cdot V \cdot (COD_0 - COD_t) / 8 \cdot I \cdot t \quad (3)$$

1
2
3

4 where COD_0 and COD_t are the initial value and the COD measured in a selected loaded
5 charge during electrolysis ($\text{g O}_2 \text{ L}^{-1}$), respectively, F is the Faraday constant (96487 C
6 mol^{-1}), V is the volume of the wastewater (L), I is the applied current (A), t is the time
7 of electrolysis (s) and 8 is the equivalent weight of oxygen. AOS variations are related
8 with the modifications that take place in the composition and in the
9 toxicity/biodegradability of the sample. COS and ACE help in estimating the efficiency
10 of the process. COS provides an estimate of the efficiency with which the carbon
11 structure of the dye molecule is degraded. The ACE value provides information on the
12 efficiency of the degradation not only of the carbon structure but also of the functional
13 groups containing heteroatoms.

14 The equation (4) was chosen for the calculus of EEO according to the report of James
15 R. Bolton (Bolton et al., 2001), considering that the concentration of initial and final
16 dyes are directly proportional to the areas of the main chromatographic peaks.
17 Therefore, the area of this peak was used in calculus instead of concentration (del Río et
18 al., 2017).

19
20
21

$$EEO=P \cdot t / V \cdot \log(A_i / A_f) \quad (4)$$

22 where: P is the electric power (kW), t is the time of electrolysis (h), V is the volume
23 treated (L), A_i and A_f are the initial and final area of the chromatographic peak
24 associated to the pollutant of interest.

1 To quantify the amount TOC and TN in a sample, analyses were performed on a
2 Shimadzu TOC-VCSN model equipped with a TNM-1 unit. The TN analysis was
3 carried out to evaluate the elimination of the triazine groups present in the structure of
4 the dyes. All samples analyzed were diluted (1:5) to obtain concentrations within the
5 operational range of the equipment. The measurements were made at 1193 K. A volume
6 of 20.0 μl of sample was injected with an air flow rate of 0.150 L min^{-1} (CO_2 free). The
7 COD measurements were performed with a MERCK TR-320 Spectroquant Thermo
8 reactor by digesting the samples with potassium dichromate and sulfuric acid. Then the
9 spectrophotometric method was applied, consistent with EPA 410.4, US Standard
10 Methods 5220 D and ISO 15705. All the reagents were supplied by Merck.

11 High Performance Liquid Chromatography (HPLC) using a Hitachi Lachrom-Elite
12 dispositive allowed the monitoring of the degradation of the samples during the
13 electrolysis. The working procedure was the procedure described in the standard EN
14 14362-2:2003/A. The measurement conditions are described in previous works (Orts et
15 al., 2018). With this procedure, the area of the chromatographic peaks associated with
16 the chromophores groups of each dye at its corresponding wavelengths was obtained.
17 Such wavelengths are 420 nm, 549 nm and 610 nm for Yellow, Crimson, and Navy,
18 respectively. The chromatographic area is in direct relation to the concentration of the
19 dye. So, we could obtain information about the amount of dye that remains in the
20 solution from its unaltered chromophore group. The evolution of these areas provides
21 information about the disappearance processes of those chromophore groups. If a
22 wavelength of 230 nm is fixed during the chromatographic analysis, the evolution of
23 aromatic structures can be studied.

24 The UV-Visible spectrophotometry measurements were performed using the same
25 chromatographic equipment Hitachi Lachrom-Elite replacing the chromatographic

1 column with a tubular piece of stainless steel without any infill inside. This device
2 allowed sample volumes of the order of μL to be analysed. The comparison of the UV-
3 Visible spectra allowed the tracking of the decolourisation from the initial to the final
4 state throughout the electrolysis, and the evolution of the functional groups and
5 aromatic structures that absorb in the UV-region.

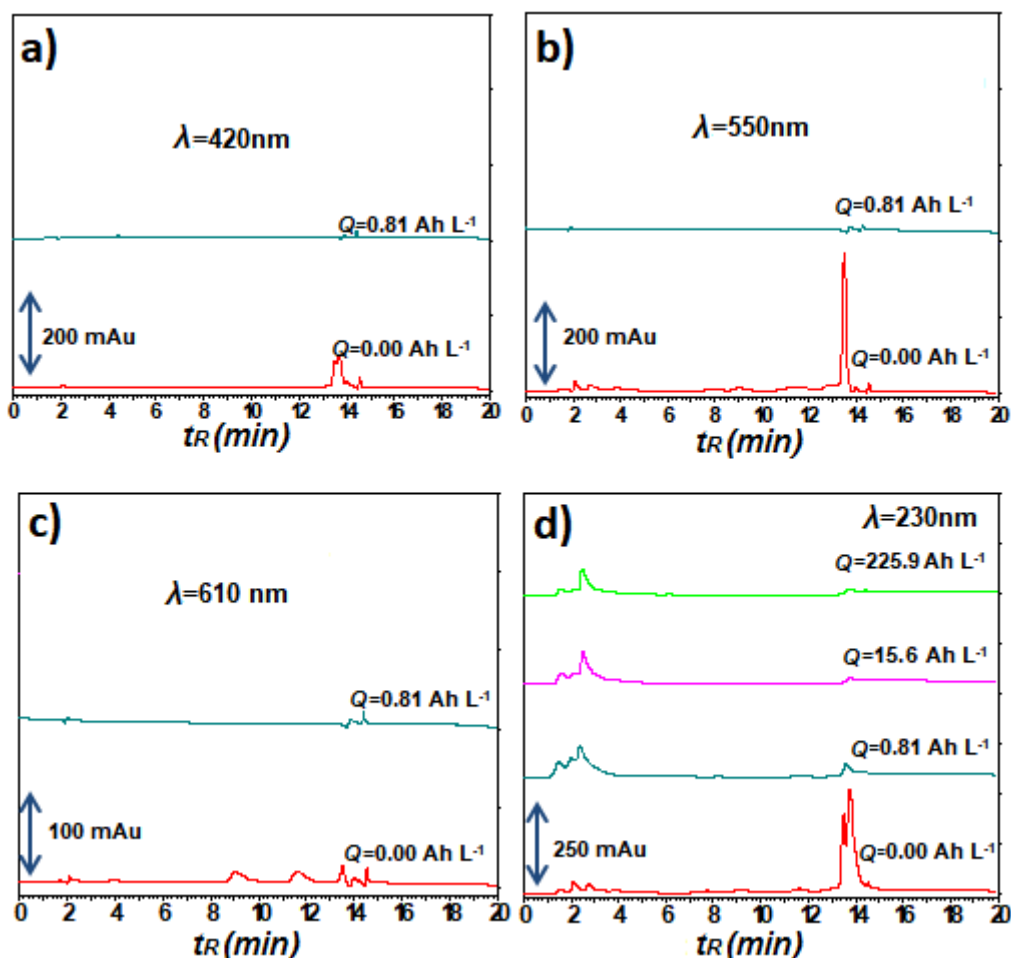
6 **3. Results and discussion**

7 *3.1. Chromatographic study*

8 Figs. 1a-c show the evolution of the chromatographic profile during the electrolysis at the
9 three wavelengths corresponding to the maximum of absorption of each dye of the
10 trichromy. The maximum loaded charge was 15.6 Ah L^{-1} because for higher load no
11 peaks are detected. In fact, at loaded charges higher than 0.81 Ah L^{-1} , an accurate
12 calculus of the area of the chromatographic peaks is not possible. For this reason, the
13 kinetic study is not shown. The results confirmed the rapid disappearance of the colour
14 of the solution during the electrolysis.

15 Fig. 1d shows the evolution of the chromatographs at a wavelength of 230 nm. The
16 initial peaks at a retention time of 13.4-13.8 min. disappear during the electrolysis. At
17 the same time, some new peaks appear at retention time of 1.0-2.0 min. These peaks
18 change their shape during the electrolysis and remain at the end of it. Thus, it seems that
19 some organic species with aromatic structure, that evolve during the electrolysis, remain
20 in solution when the process finishes.

21



1

2 **Fig. 1.** Evolution of the chromatographic profile during the electrolysis using chloride as
 3 electrolyte (30.0 g L^{-1}) at the maximum absorpition wavelegh of: a) Procion Yellow. b) Procion
 4 Crimson. c) Procion Navy. d) Aromatic structures. The initial concentration of each dye was
 5 0.50 g L^{-1} . The applied current density was 125 mA cm^{-2} and the volume of electrolysed sample
 6 was 0.45 L .

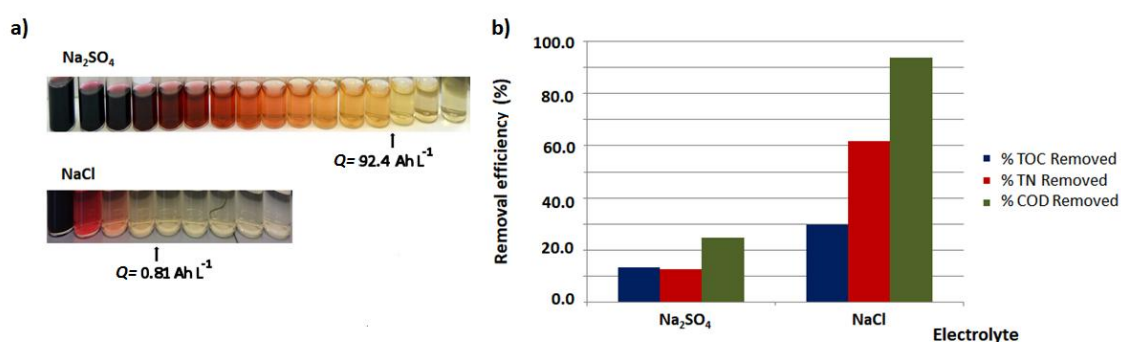
7

8 *3.2. Comparative study of the evolution of electrolysis parameters in sulphate and*
 9 *chloride media.*

10

11 Fig. 2a shows the photography of different samples extracted during the electrolysis
 12 with sulphate and chloride. A visual inspection is enough to conclude that the loaded
 13 charge needed for decolourisation drastically decreased in the case of chloride. Fig. 2b
 14 shows the decrease in TOC, COD and TN for both electrolytes at a similar loaded
 15 charge to that needed for total decolourisation in sulphate medium (to ensure similar
 16 experimental conditions) (Orts et al. 2018). The removal efficiency is higher in the

1 presence of chloride, particularly in the decrease of TN and COD. This higher
2 efficiency is due to the fact that, in the electrolysis, chloride is oxidized giving rise to
3 highly oxidizing species (such as hypochlorite or hypochloric acid, depending on the
4 pH) (García Segura et al., 2018). These species are those that subsequently react with
5 the organic pollutant to degrade it acting as electroactive substances mediating the
6 electronic transfer. In both cases the elimination of COD is greater than that of TOC and
7 TN. This involves the generation of fairly oxidized species that remain stable in
8 solution.



9
10

11 **Fig. 2.** a) Photography of samples extracted during the electrolysis with sulphate (45.0 g L^{-1}) or
12 chloride (30.0 g L^{-1}) as electrolytes. The loaded charge needed in each decolourisation is shown
13 in Figure b) Removal efficiency (%) of TOC, TN and COD with sulphate or chloride as
14 electrolyte, after a loaded charge of around the needed for total decolourisation in sulphate
15 medium. The initial concentration of each dye was 0.50 g L^{-1} . The applied current density was
16 125 mA cm^{-2} and the volume of electrolysed sample was 0.45 L . The flow rate was 5.60 L min^{-1} .
17

18
19

20 Moreover, Table 1 shows the values of %TOC, %TN and %COD removed at
21 different values of loaded charge. At a loaded charge in which decolourisation occurs in
22 chloride medium (0.81 Ah L^{-1}) the %TN and %TOC removed are high. So, in the first
23 stage of electrolysis, not only the chromophore groups are degraded but also,
nitrogenated groups (such as chlorotriazines) are removed from the molecular structure

1 and, subsequently, the carbon atoms present in its structure. This will be corroborated
2 by the spectroscopic results.

3 **Table 1**

4 Values of %TOC, %TN and %COD removed at different values of loaded charge, with both
5 chloride and sulphate electrolytes.

6

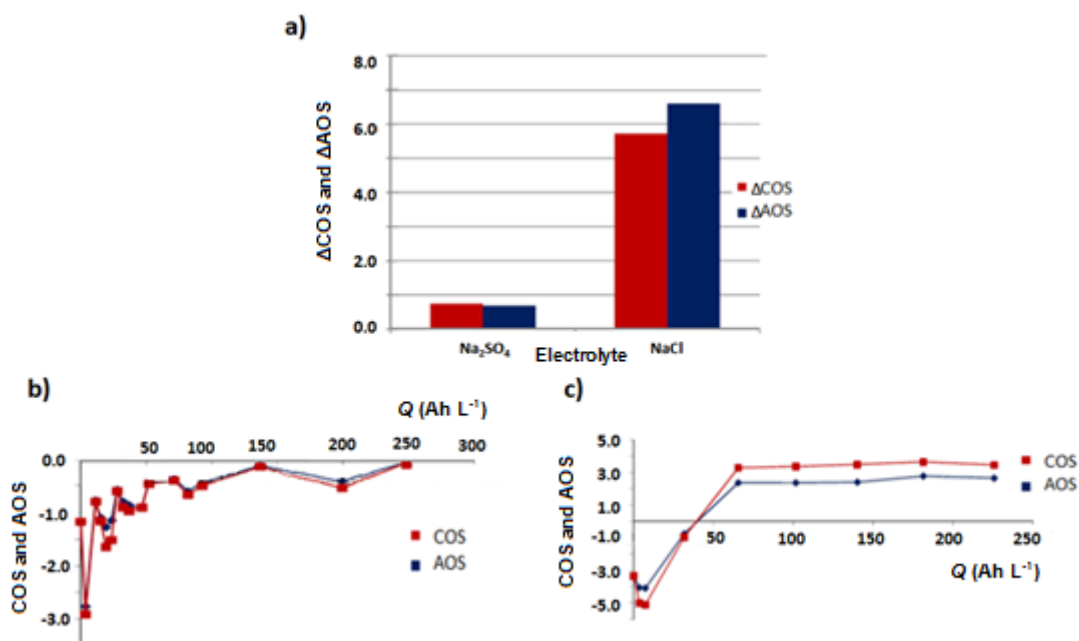
ELECTROLYTE	Q (Ah L ⁻¹)	%TOC	%TN	%COD
NaCl	0.81	19.1	33.4	0.87
	101.7	29.7	61.8	93.9
Na ₂ SO ₄	92.4	13.3	12.7	24.8

7

8 Fig. 3a shows the variation of COS and AOS with sulphate (Orts et al. 2018) or
9 chloride as electrolyte, after a loaded charge corresponding to that needed for total
10 decolourisation in sulphate medium. Positive trends in AOS relative to the initial value
11 indicate that the final compounds are more oxidized than the untreated dye molecules
12 (del Río et al., 2009a). Changes in COS values are related to changes in the composition
13 of the solution as a result of electrochemical treatment. For both electrolytes an increase
14 in COS and AOS values were observed, although this variation is much more
15 pronounced in the presence of chloride. Fig. 3b-c show the evolution of COS and AOS
16 with loaded charge during the electrolysis with sulphate (Orts et al. 2018) and chloride
17 as electrolytes, respectively. The evolution of both parameters occurs in a more
18 pronounced way with chloride. At the beginning of the electrolysis, COS and AOS
19 increase, so, oxidation occurs changing the oxidation state of the dye. Later COS and
20 AOS remain practically constant. Therefore, can be concluded that the electrolysis
21 continues oxidising and mineralising the samples and that both processes take place at
22 similar rate.

23

24



1
2

Fig. 3. a) Variation of COS and AOS with sulphate (45.0 g L^{-1}) or chloride (30.0 g L^{-1}), after a loaded charge corresponding to the need for total decolourisation in sulphate medium. b) Evolution of COS and AOS with loaded charge during the electrolysis with sulphate as electrolyte. c) Evolution of COS and AOS with loaded charge during the electrolysis with chloride as electrolyte. The initial concentration of each dye was 0.50 g L^{-1} . The applied current density was 125 mA cm^{-2} and the volume of electrolysed sample was 0.45 L . The flow rate was 5.60 L min^{-1} .

10
11
12
13

The average current efficiency (ACE) indicates the fraction of current that has been used to decrease COD by a certain percentage, while COS provides information on the efficiency with which the carbon structure of the dye is degraded. The ACE values provide an estimate of the degradation efficiency of the whole molecule. For a loaded charge similar to that needed for total decolourisation in sulphate medium, the value of ACE is 1.4% whereas in similar loaded charge conditions, the ACE value in chloride medium increases up to 5.6%. When the electrolysis process passes from the decolourisation stage increasing the loaded charge values, there is a decrease in the percentage of ACE during the time of electrolysis. For instance, for a value of loaded charge of around 230 Ah L^{-1} , the percentages of ACE were 2.5% and 0.97% with

1 chloride and sulphate, respectively. This could be because in the initially stages of the
2 electrolysis, the main reactions are the degradation of chromophores and reactive groups
3 of dye molecules. But, as their concentration decreases, they give way to more complex
4 degradation reactions and to water electrolysis. This is consistent with the spectroscopic
5 results. Nevertheless, the process continues being more efficient in the presence of
6 chlorides by the generation of chloride oxidation products during the electrolysis.

7

8 As a consequence of the increase in efficiency and the faster decolourisation
9 observed when chloride electrolyte is used, the Electrical Energy per Order (EEO)
10 decreased significantly. Thus, after total decolourisation the value of EEO obtained is
11 1.2 kWh m^{-3} with chloride and 152.0 kWh m^{-3} with sulphate.

12

13 *3.4. Evolution of the UV-Vis spectra*

14

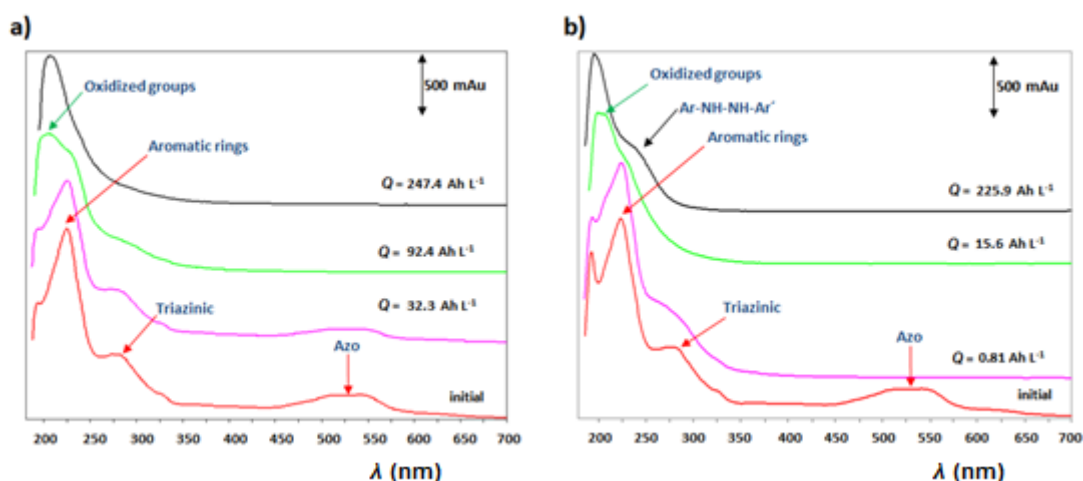
15

16 Figs. 4a-b show the UV-Vis spectra evolution during the electrolysis with sulphate
17 (Orts et al. 2018) and chloride as electrolytes, respectively. In the initial spectra, bands
18 associated with the azo groups are observed. These bands are around 420 nm, 549 nm,
19 and 610 nm for Procion Yellow, Procion Crimson, and Procion Navy, respectively.
20 These bands quickly disappear in the presence of chloride while in the case of sulphate
21 a higher loaded charge (higher than 0.81 Ah L^{-1}) is needed. These results confirmed the
22 HPLC results.

23

24

25



1
2 **Fig. 4.** UV-Vis spectra evolution of a) during electrolysis with sulphate (45.0 g L^{-1}) as electrolyte.
3 b) During electrolysis with chloride (30.0 g L^{-1}) as electrolyte. The initial concentration of each
4 dye was 0.50 g L^{-1} . The applied current density was 125 mA cm^{-1} .

5
6 The band centered at 280 nm (triazinic groups) (Chapman, 2005) completely
7 disappears during electrolysis, which is also confirmed by the decrease of TN. The band
8 at 230 nm ($\pi \rightarrow \pi^*$ transitions of benzenic and naphthalenic rings) (Stylidi et al., 2004)
9 diminishes indicating a loss of aromaticity. Although in the presence of sulphate this
10 band is still detected, in the presence of chloride it completely disappears. At the end of
11 the electrolysis in presence of chlorides, two bands corresponding to the Ar-NH-NH-
12 Ar' structure (Feng et al., 2000), at 245 nm is clearly noted. A $\pi \rightarrow \pi^*$ transition at 210
13 nm of highly oxidized groups, such as carbonyl (Chapman, 2005) is also observed.

14 From all these results, an oxidation/reduction reaction mechanism with chloride and
15 sulphate as electrolyte is shown in Fig. 5.

16

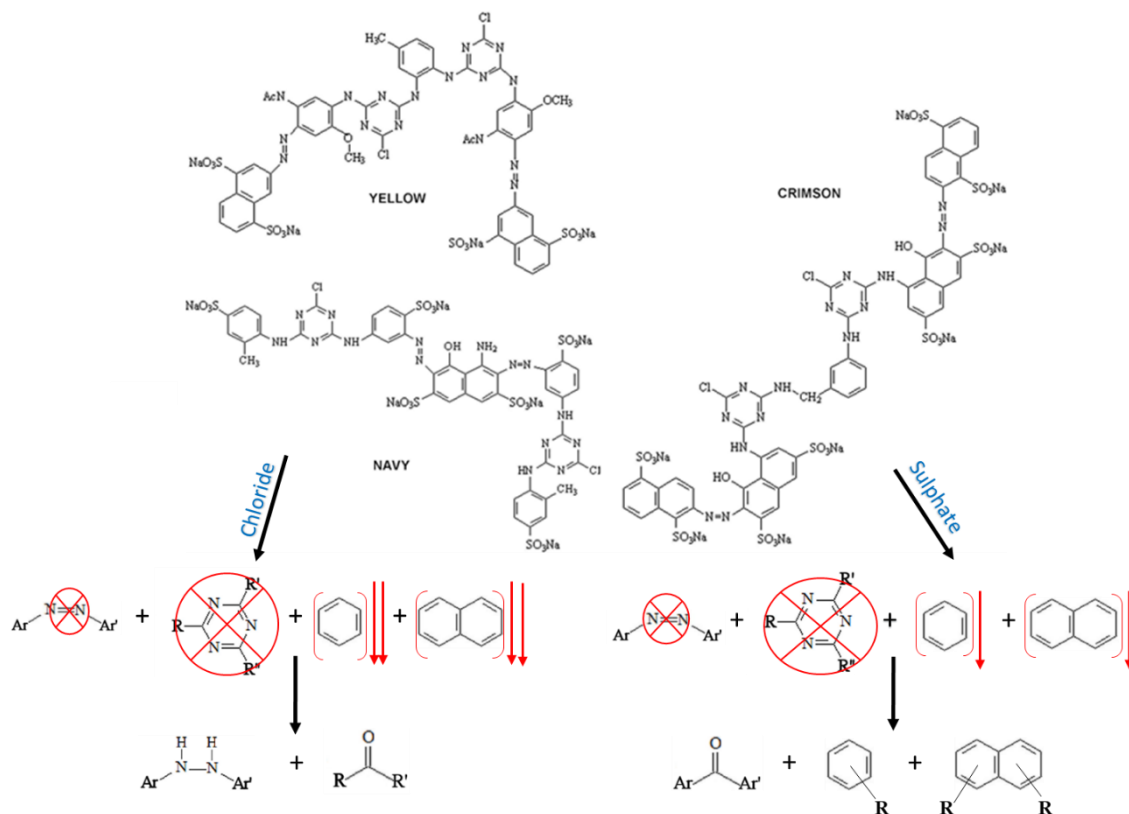


Fig. 5: Oxidation/reduction reaction mechanism with chloride and sulphate as electrolyte.

3.5. Reuse experiments

In contrast with what occurred when sulphate is used (Orts et al., 2018, 2019), the evaluation of colour matching after dyeing processes with the reusing water from the electrolysis in the presence of chloride, gives values outside the limits accepted in the textile industry. The evolution of the composition of the electrolyzed solution due to the presence of oxidation intermediates of chloride whose nature and concentration changes with time and the appearance of photochemical reactions may be the reason for this behavior (López Grimau and Gutiérrez, 2006). This is not to say that the reuse water cannot be used in dyeing processes, but simply that for the requirements of the colour matching, the reused water requires a treatment with UV-light to eliminate the

1 remains of chlorinated species. It is also possible to adjust the initial quantities of dye
2 used in the dyeing process to match the requirements of colour matching.

3

4 **4. Conclusions**

5

6

7

8 In the present work the results obtained using sulphate or chloride as electrolyte in
9 the electrolysis of real textile wastewater after dyeing with the trichromy Procion
10 HEXL cotton yarns are compared. As anode, a DSA electrode of Ti-SnO₂-Sb-Pt was
11 used and as cathode a stainless steel plate was selected. As shown in previous studies,
12 when sulphate is chosen as electrolyte, a moderate decrease of COD, TOC, and TN
13 together with a complete decolourisation was obtained. Moreover, a good colour
14 matching in the successive dyeing was also obtained. So, it can be concluded that in the
15 presence of sulphate reuse is possible, saving water and electrolyte. Nevertheless, the
16 loaded charge needed for that purpose, and as such, the electrical energy per order are
17 high and the current efficiency is poor.

18 In the other hand, the results obtained in the present work show a higher degradation
19 of organic matter, rapid decolourisation, better current efficiency, and lower energy
20 consumption (1.2 kWh m⁻³) when chloride is used as electrolyte. Nevertheless, the
21 elimination of COD is greater than that of TOC and TN. This indicates the generation of
22 fairly oxidized carbon and nitrogen species that remain stable in the solution. The
23 efficiency of the process in terms of oxidation and mineralisation can be assessed by
24 analyzing the variation of carbon oxidation state (COS) and the variation of the average
25 oxidation state (AOS). These variations are always higher than in the case of using
26 sulphate and the results indicate that in a first phase both parameters continuously
27 increase which means that the oxidation mainly occurs rather than mineralisation.

1 Subsequently, a second phase of the experiments showed that COS and AOS remain
2 constant. This implies that, although the process is able to continue to oxidize and
3 mineralize the sample, both processes happen at similar rates. Moreover, it is possible to
4 use reused wastewater when chloride is used as electrolyte in dyeing processes. To
5 comply with the textile industry requirements of colour matching, two successful
6 strategies are possible: Pretreatment of the reused wastewater with UV-light to
7 eliminate the remains of chlorinated species or modifying the proportions of the initial
8 quantity of dyes used in the dyeing process.

9
10

11 **Acknowledgments**

12

13 The authors wish to thank the Spanish Agencia Estatal de Investigación (AEI) and European
14 Union (FEDER funds) for the financial support (contract MAT2016-77742-C2-1-P and Red
15 E3Tech CTQ2017-90659-REDT). The authors wish to acknowledge Tim Vickers for help with
16 the English revision and Texcoy S.L. company (Spain) where the dyeing processes were done.

17
18
19

20 **References**

21

22 Akrou, H., Bousselmi, L., 2012. Chloride ions as an agent promoting the oxidation of
23 synthetic dyestuff on BDD electrode. *Desalin. Water Treat.* 46, 171–181.

24 <https://doi.org/10.1080/19443994.2012.677528>

25 Allen, R.L.M., 1971. *Colour Chemistry*. Springer US, Boston, MA.

26 <https://doi.org/10.1007/978-1-4615-6663-2>

27 Bilińska, L., Gmurek, M., Ledakowicz, S., 2016. Comparison between industrial and
28 simulated textile wastewater treatment by AOPs – Biodegradability, toxicity and

1 cost assessment. Chem. Eng. J. 306, 550–559.
2 <https://doi.org/10.1016/J.CEJ.2016.07.100>

3 Blanco, J., Torrades, F., Morón, M., Brouta-Agnésa, M., García Montaña, J., 2014.
4 Photo-Fenton and sequencing batch reactor coupled to photo-Fenton processes for
5 textile wastewater reclamation: Feasibility of reuse in dyeing processes. Chem.
6 Eng. J. 240, 469–475.
7 <https://doi.org/10.1016/J.CEJ.2013.10.101>

8 Bolton, J.R., Bircher, K.G., Tumas, W., Tolman, C.A., 2001. Figures of merit for the
9 technical development and application of advanced oxidation technologies for both
10 electric and solar driven systems (IUPAC Technical Report). Pure Appl. Chem. 73,
11 627–637.
12 <https://doi.org/10.1351/pac200173040627>

13 Brillas, E., Martínez-Huitle, C.A., 2015. Decontamination of wastewaters containing
14 synthetic organic dyes by electrochemical methods. An updated review. Appl.
15 Catal. B Environ. 166–167, 603–643.
16 <https://doi.org/10.1016/J.APCATB.2014.11.016>

17 Carneiro, P.A., Osugi, M.E., Fugivara, C.S., Boralle, N., Furlan, M., B. Zanoni, M.V.,
18 2005. Evaluation of different electrochemical methods on the oxidation and
19 degradation of Reactive Blue 4 in aqueous solution. Chemosphere 59, 431–439.
20 <https://doi.org/10.1016/j.chemosphere.2004.10.043>

21 Chapman, O.L., 2005. Spectrometric Identification of Organic Compounds. J. Am.
22 Chem. Soc. 85, 3316–3316.

1 <https://doi.org/10.1021/ja00903a077>

2 Comninellis, Ch., Pulgarin, C., 1991. Anodic oxidation of phenol for waste water
3 treatment. *J. Appl. Electrochem.* 21, 703–708.

4 <https://doi.org/10.1007/BF01034049>

5 De Jager, D., Sheldon, M.S., Edwards, W., 2014. Colour removal from textile
6 wastewater using a pilot scale dual stage MBR and subsequent RO system. *Sep.*
7 *Purif. Technol.* 135, 135–144.

8 <https://doi.org/10.1016/j.seppur.2014.08.008>

9 del Río, A.I., Orts, F., Molina, J., Bonastre, J.A., Cases, F., 2012. Tratamiento
10 electroquímico de colourantes bifuncionales tipo HEXL en un reactor filtro prensa.
11 *Dyna* 87, 679–688.

12 <https://doi.org/10.6036/4682>

13 del Río, A.I., Fernández, J., Molina, J., Bonastre, J., Cases, F., 2010. On the behaviour
14 of doped SnO₂ anodes stabilized with platinum in the electrochemical degradation
15 of reactive dyes. *Electrochim. Acta* 55, 7282–7289.

16 <https://doi.org/10.1016/j.electacta.2010.07.008>

17 del Río, A.I., García, C., Molina, J., Fernández, J., Bonastre, J., Cases, F., 2017. On the
18 behavior of reduced graphene oxide based electrodes coated with dispersed
19 platinum by alternate current methods in the electrochemical degradation of
20 reactive dyes. *Chemosphere* 183, 242–251.

21 <https://doi.org/10.1016/j.chemosphere.2017.05.121>

22 del Río, A.I., Molina, J., Bonastre, J., Cases, F., 2009a. Study of the electrochemical

1 oxidation and reduction of C.I. Reactive Orange 4 in sodium sulphate alkaline
2 solutions. *J. Hazard. Mater.*
3 <https://doi.org/10.1016/j.jhazmat.2009.06.147>

4 del Río, A.I., Molina, J., Bonastre, J., Cases, F., 2009b. Influence of electrochemical
5 reduction and oxidation processes on the decolourisation and degradation of C.I.
6 Reactive Orange 4 solutions. *Chemosphere.*
7 <https://doi.org/10.1016/j.chemosphere.2009.02.063>

8 Drumond Chequer, F.M., de Oliveira, G.A.R., Anastacio Ferraz, E.R., Carvalho, J.,
9 Boldrin Zanoni, M.V., de Oliveir, D.P., 2013. Textile Dyes: Dyeing Process and
10 Environmental Impact, in: *Eco-Friendly Textile Dyeing and Finishing*. InTech.
11 <https://doi.org/10.5772/53659>

12 Eaton, A. D., L. S. Clesceri, and A.E.G., 1995. *Standard Methods for the Examination*
13 *of Water and Wastewater*, 9th ed [WWW Document]. Am. Public Heal. Assoc.
14 Washington, D.C. URL <https://www.standardmethods.org/> (accessed 3.7.19).

15 European Comission, 2005. *Best Available Techniques in the Slaughterhouses and*
16 *Animal By-products Industries*, Institute for Prospective Technological Studies
17 European IPPC Bureau.

18 Feng, W., Nansheng, D., Helin, H., 2000. Degradation mechanism of azo dye C. I.
19 reactive red 2 by iron powder reduction and photooxidation in aqueous solutions.
20 *Chemosphere* 41, 1233–1238. [https://doi.org/10.1016/S0045-6535\(99\)00538-X](https://doi.org/10.1016/S0045-6535(99)00538-X)

21 Fóti, G., Comninellis, Ch., 2010. *Electrochemistry for the Environment*, in: Springer,
22 N.Y. (Ed.), *Electrochemistry for the Environment*. pp. 1–23.
23 <https://doi.org/10.1007/978-0-387-68318-8>

- 1 Ghaly, A.E., Ananthashankar, R., Alhattab, M., Ramakrishnan, V.V., 2014. Production,
2 Characterization and Treatment of Textile Effluents: A Critical Review. *J. Chem.*
3 *Eng. Process Technol.* 5, 1–18.
4 <https://doi.org/10.4172/2157-7048.1000182>
- 5 García Segura, S., Ocon, J.D., Chong, M.N., 2018. Electrochemical oxidation
6 remediation of real wastewater effluents — A review. *Process Saf. Environ. Prot.*
7 113, 48–67.
8 <https://doi.org/10.1016/j.psep.2017.09.014>
- 9 Guaratini, C.C.I., Fogg, A.G., Zanoni, M.V.B., 2001a. Studies of the voltammetric
10 behavior and determination of diazo reactive dyes at mercury electrode.
11 *Electroanalysis* 13, 1535–1543.
12 [https://doi.org/10.1002/1521-4109\(200112\)13:18<1535::AID-](https://doi.org/10.1002/1521-4109(200112)13:18<1535::AID-ELAN1535>3.0.CO;2-H)
13 [ELAN1535>3.0.CO;2-H](https://doi.org/10.1002/1521-4109(200112)13:18<1535::AID-ELAN1535>3.0.CO;2-H)
- 14 Guaratini, C.C.I., Fogg, A.G., Zanoni, M.V.B., 2001b. Assessment of the application of
15 cathodic stripping voltammetry to the analysis of diazo reactive dyes and their
16 hydrolysis products. *Dye. Pigment.* 50, 211–221.
17 [https://doi.org/10.1016/S0143-7208\(01\)00050-X](https://doi.org/10.1016/S0143-7208(01)00050-X)
- 18 Jarrah, N., Mu'azu, N.D., 2016. Simultaneous electrooxidation of phenol, CN⁻, S²⁻
19 and NH₄⁺ in synthetic wastewater using boron doped diamond anode. *J. Environ.*
20 *Chem. Eng.* 4, 2656–2664.
21 <https://doi.org/10.1016/J.JECE.2016.04.011>

22

- 1 Lacasse, K., Baumann, W., 2012. Textile Chemicals: Environement data and facts,
2 Springer.
- 3 Li, P., Cai, W., Xiao, Y., Wang, Y., Fan, J., 2017. Electrochemical Degradation of
4 Phenol Wastewater by Sn-Sb-Ce Modified Granular Activated Carbon. *Int. J.*
5 *Electrochem. Sci* 12, 2777–2790.
6 <https://doi.org/10.20964/2017.04.58>
- 7 Ling, Y., Hu, J., Qian, Z., Zhu, L., Chen, X., 2016. Continuous treatment of biologically
8 treated textile effluent using a multicell electrochemical reactor. *Chem. Eng. J.*
9 286, 571–577.
10 <https://doi.org/10.1016/j.cej.2015.10.104>
- 11 López Grimau, V., Gutiérrez, M.C., 2006. Decolourisation of simulated reactive
12 dyebath effluents by electrochemical oxidation assisted by UV light. *Chemosphere*
13 62, 106–112.
14 <https://doi.org/10.1016/j.chemosphere.2005.03.076>
- 15 Malpass Geoffroy, R.P., Andresa Mortari, D., Miwa, D., Machado, S.A.S., Motheo,
16 A.J., 2007. Decolourisation of Real Textile Waste Using Electrochemical
17 Techniques: Effect of the Chloride Concentration. *Water Res.* 41, 2969–2977.
18 <https://doi.org/10.1016/j.watres.2007.02.054>
- 19 Martínez-Huitle, C.A., Brillas, E., 2009. Decontamination of wastewaters containing
20 synthetic organic dyes by electrochemical methods: A general review. *Appl. Catal.*
21 *B Environ.* 87, 105–145.
22 <https://doi.org/10.1016/j.apcatb.2008.09.017>

- 1 Martínez-Huitle, C.A., Dos Santos, E.V., De Araújo, D.M., Panizza, M., 2012.
2 Applicability of diamond electrode/anode to the electrochemical treatment of a real
3 textile effluent. *J. Electroanal. Chem.* 674, 103–107.
4 <https://doi.org/10.1016/j.jelechem.2012.02.005>
- 5 Miklos, D.B., Remy, C., Jekel, M., Linden, K.G., Drewes, J.E., Hübner, U., 2018.
6 Evaluation of advanced oxidation processes for water and wastewater treatment –
7 A critical review. *Water Res.* 139, 118–131.
8 <https://doi.org/10.1016/J.WATRES.2018.03.042>
- 9 Moreira, F.C., Boaventura, R.A.R., Brillas, E., Vilar, V.J.P., 2017. Electrochemical
10 advanced oxidation processes: A review on their application to synthetic and real
11 wastewaters. *Appl. Catal. B Environ.*
12 <https://doi.org/10.1016/j.apcatb.2016.08.037>
- 13 Orts, F., del Río, A.I., Molina, J., Bonastre, J., Cases, F., 2018. Electrochemical
14 treatment of real textile wastewater: Trichromy Procion HEXL®. *J. Electroanal.*
15 *Chem.* 808, 387–394.
16 <https://doi.org/10.1016/J.JELECHEM.2017.06.051>
- 17 Orts, F., Del Río, A.I., Molina, J., Bonastre, J., Cases, F., 2019. Study of the Reuse of
18 Industrial Wastewater After Electrochemical Treatment of Textile Effluents
19 without External Addition of Chloride. *Int. J. Electrochem. Sci.* 14, 1733–1750.
20 <https://doi.org/10.20964/2019.02.27>
- 21 Sala, M., del Río, A.I., Molina, J., Cases, F., Gutiérrez Bouzán, M.C., 2012. Influence
22 of Cell Design and Electrode Materials on the Decolouration of Dyeing Effluents,
23 *Int. J. Electrochem. Sci.* 7, 12470–12488.

- 1 Sala, M., Gutiérrez Bouzán, M.C., 2014. Electrochemical treatment of industrial
2 wastewater and effluent reuse at laboratory and semi-industrial scale. *J. Clean.*
3 *Prod.* 65, 458–464.
4 <https://doi.org/10.1016/j.jclepro.2013.08.006>
- 5 Shukla, S.R., 2007. Pollution abatement and waste minimisation in textile dyeing, in:
6 *Environmental Aspects of Textile Dyeing*. pp. 116–148.
7 <https://doi.org/10.1533/9781845693091.116>
- 8 Stumm, W., Morgan, J., 2013. Aquatic chemistry: chemical equilibria and rates in
9 natural waters. *Choice Rev. Online* 33, 33-6312-33–6312.
10 <https://doi.org/10.5860/choice.33-6312>
- 11 Stylidi, M., Kondarides, D.I., Verykios, X.E., 2004. Visible light-induced photocatalytic
12 degradation of Acid Orange 7 in aqueous TiO₂ suspensions. *Appl. Catal. B*
13 *Environ.* 47, 189–201.
14 <https://doi.org/10.1016/j.apcatb.2003.09.014>
- 15 Tarr, M.A., 2003. *Chemical Degradation Methods for Wastes and Pollutants:*
16 *Environmental and Industrial Applications*, ed. Matthew A. Tarr, University of
17 New Orleans, New Orleans, Louisiana, U.S.A.
- 18 Xu, M., Wang, Z., Wang, F., Hong, P., Wang, C., Ouyang, X., Zhu, C., Wei, Y., Hun,
19 Y., Fang, W., 2016. Fabrication of cerium doped Ti/nanoTiO₂/PbO₂ electrode
20 with improved electrocatalytic activity and its application in organic degradation.
21 *Electrochim. Acta* 201, 240–250.
22 <https://doi.org/10.1016/J.ELECTACTA.2016.03.168>

